ARTIKEL RISET

The Study of Seeing Characteristic at the UAD Observatory on Procyon, Sirius, Spica, Nunki, Altair, and Vega using a 150 mm diameter Celestron C6-N telescope

Ricka Tanzilla, Yudhiakto Pramudya*, M. Khairul Ardi and Okimustava

Received: July 24, 2020 | Accepted: August 31, 2020 | Published: Sept 17, 2021 | **DOI**: 10.22146/jfi.v25i1.58087

Abstract

Astronomical observatories can be declared feasible if they have a good condition such as a dark sky, relatively little cloud coverage, relatively low light pollution, and small air turbulence or seeing. The UAD (Universitas Ahmad Dahlan) observatory was measuring the seeing characteristic to assess the feasibility condition. The DIMM method (Differential Image Motion Monitor) was utilized to get the measurement in April, May, and September 2019. The 150 mm diameter Celestron C6-N telescope was used as the instrument to get the star images. The characteristics of a good seeing value on April 10, 2019, are Procyon star with a value of 0.2 arc seconds, and on September 18, 2019, the Vega star with a value of 1.6 arc seconds. Analysis of the seeing characteristic at the UAD Observatory can be used as a reference for observers on star selection, and the operation of the telescope.

Keywords: Seeing; DIMM; Observatory; Turbulence; Atmosphere.

1 INTRODUCTION

The observatory requires a low light pollution and a high quality of meteorological conditions at the site. The atmospheric condition will affect the path of starlight into the telescope. At the point of the light source in the sky has a parallel wave front will be distorted when entering the Earth's atmosphere, resulting in spatial and temporal variations in the refractive index along the path to the surface of the Earth. This effect is known as seeing [1]. Seeing is defined as the full width at half maximum (FWHM) star images at the focus of large diameter telescopes and for observations at zenith [2]. The single parameter used to determine the FWHM image implicitly assumes that energy flowed into the atmosphere at an infinite scale follows Kolmogorov's turbulence model [3].

A telescope has a resolution that is proportional to λ/D (λ is the wavelength of electromagnetic radiation and D is the diameter of the telescope). In a large diameter telescope, the atmospheric turbulent limiting the angle of resolution of an image produced during observation [4, 5]. Most observatories are able to monitor the quality of the atmosphere in seeing even though it is often in poor viewing conditions [5, 6, 7]. Universitas Ahmad Dahlan (UAD) Observatory is located at Jl. Ringroad Selatan, Kragilan, Tamanan, Banguntapan, Bantul, which coordinate of -7.83^o Latitude and 110.38^o Longitude. UAD Observatory had conducted several astronomical studies, for example, measuring the eccentricity of the Moon's orbit [8], the phases of the Moon that influenced the initial determination of astronomical dawn in Yogyakarta [9]. Observatories are important to provide detailed observational conditions such as seeing conditions and the brightness of the sky as a reference for astronomers. This study will focus on the characteristics of seeing value at the UAD observatory using the Differential Image Motion Monitor (DIMM) method with the 150 mm Celestron C6-N telescope. The target stars are Procyon, Sirius, Spica, Nunki, Altair, and Vega. They were observed when in the

*Correspondence: *yudhiakto.pramudya@pfis.uad.ac.id*
Magister Pendidikan Fisika, Universitas Ahmad Dahlan, Yogyakarta, Indonesia
Full list of author information is available at the end of the article
†Equal contributor

vicinity of zenith distance ($z < 30^o$) with the absolute magnitude of 2.68, 1.47, -3.55, -2.14, 2.21, and 0.58, respectively.

2 SEEING

Seeing is the turbulence effect of the Earth's atmosphere. The atmosphere contains gas, liquid, and solid particle gases. The layers of atmosphere differ in size from tens of centimeters to meters. Each layer has a different refractive index. The difference between the refractive indexes of cells is only one-tenth. Earth's atmosphere can be treated similar to a lens system. Wave front from celestial objects will change its shape as they pass through Earth's atmosphere [5, 10]. Earth's atmosphere has variations in pressure and temperature, causing changes in the refractive index as the light entering from the star to the telescope. This atmospheric turbulence causes the intensity of the received signal and phase fluctuations resulting in blurred images [11].

3 KOLMOGOROV'S THEOREM ON TURBULENT

Turbulence is a phenomenon in fluid dynamic systems characterized by chaotic velocity fields. The general definition of turbulence is a state of ongoing instability, such as atmospheric circulation [12]. Research on turbulence can involve people from various disciplines such as applied mathematics, physics, chemistry, and engineering [13],Kusuma2007.

In 1941, A.N. Kolmogorov put forward Kolmogorov's theorem. He concluded that turbulent flow shows that the amount of energy supplied can be assumed to be the same as the amount of energy dissipated at a specific rate [14]. Thus, one basic theory of turbulent flow is Kolmogorov's theory, which states that velocity fluctuations are assumed to occur universally. The amount of energy is assumed to depend only on turbulent dissipation [5, 15].

4 RELATIONSHIP BETWEEN KOLMOGOROV'S THEOREM WITH SEEING

The basic hypothesis of Kolmogorov's theory is the shape of the phase structure-function, the average of the differential phase error between the points separated by distance r. The phase structure function is

$$D_\phi(r) = 6.88 \left(\frac{r}{r_o}\right)^{5/3} \tag{1}$$

with a constant proportional to r_o giving a value of certain seeing quality [16]. Coherent length r_o (also known as the Fried Parameter) [17]. The equation used to calculate seeing from motion image variance is published by (Martin, 1987) and (Fried, 1965). The variance of differential image motion $(\sigma_d)^2$ is related to the Fried r_o parameter, wavelength λ, and K are constants. By substituting equation (1) into equation (2), we get the variance of differential image motion $(\sigma_d)^2$ (in radians squared).

$$\sigma_d^2 = K\lambda^2 r_o^{-5/3} D_\phi^{-1/3} \tag{2}$$

The units λ, r_o, D_Φ are centimeters. In the exposure of a large diameter telescope, an image of a star will produce (FWHM) can be seen from equation (3).

$$FWHM = 0.98 \left(\frac{D_\phi}{\lambda}\right)^0 .2 \left(\frac{\lambda_d^2}{K}\right)^0 .6 \tag{3}$$

Seeing is dominant when $r_o < D_\Phi$, hence that higher r_o means better seeing [18].

5 FWHM (Full Width at Half Maximum)

FWHM is a characteristic of a function or graph curve and explains how broad the distribution data is [19]. FWHM was applied to phenomena such as pulse waveform duration and source spectral width used for optical communication and spectrometer resolution [20]. FWHM on a long exposure of star images is the nature of images obtained by the focal plane of the instrument mounted on the telescope observed through the atmosphere. Regardless of instrument deviations, one of the turbulence properties that affects image quality is the largest turbulent vortex size in the atmosphere [21]. FWHM can be employed for seeing from pictures of stars at the focus of large diameter telescopes and observations at zenith. FWHM is given by [18]

$$FWHM = 0.98 \frac{\lambda}{r_o} \tag{4}$$

where λ is the wavelength, and r_o is the Fried Parameter.

6 DIMM (Differential Image Motion Monitor)

The most common way to determine the quality of seeing is by measuring the star's FWHM image at the focus of the telescope. However, such measurements include "blurred" or momentary image expansion and "motion picture" or erratic image movement

[22, 23]. There are several methods used to determine the value of seeing. Nevertheless, some of these methods usually experience drive errors and telescopic vibrations contribute to image motion [16].

DIMM (Differential Image Motion Monitor) is a technique that has been universally accepted for measuring seeing [7, 18]. The concept of seeing was introduced by Stock and Keller in 1960 [24]. It is also explained by Sarazin and Roddier [25]. The principle of the DIMM technique is to measure the displacement of the position of an artificial double star made by two sub-aperture telescopes. The principle of the DIMM technique is to measure the displacement of the position of an artificial double star made by two sub-aperture telescopes. Two sub-aperture telescopes are only made using a two-hole mask placed at the telescope's aperture.

7 METHODS

The research method is an observation using a Celestron C6-N telescope with a diameter of 150 mm. The telescope is equipped with Celestron Skyris CCD 236 m and a camera resolution of 1600 × 1200 Pixels. We tracked the star image in a video to get the position as a function of time. The video will be analyzed using the DIMM technique. The video resolution is 20 frames per second. Every video has no editing process. The observation is designed to be performed on the dry season in Indonesia to get more chance of clear sky.

The observation set up is shown in figure 7. A mask covers the objective part of the telescope. There are two holes on the mask. The diameter of a hole (D) is 3 cm. The distance between two centers of holes (d) is 12 cm.

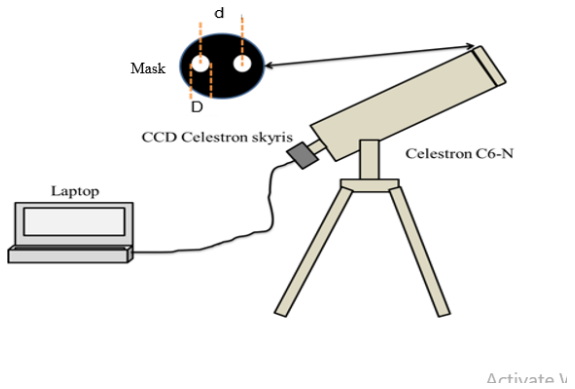

Figure 1: Scheme of observation instrument setup.

The video was analyzed by using a tracker to get the position of the star image as a function of time. Data analysis was performed to measure seeing using the DIMM technique. In the DIMM technique, it is as if there are two "stars" formed from a beam of light entering through each hole in the mask. Atmospheric turbulence will cause the distance of the two "stars" to be seen to change. Hence, there is a longitudinal and transverse direction. The longitudinal direction (1) in the direction parallel to the connecting lines of the two holes and the transverse direction (t) is the direction perpendicular to the connecting lines of the two holes. Variations in the distance of the two "stars" can be written as follows [25]:

$$\sigma_l^2 = 2\lambda^2 r_o^{5/3} \left[0.179D^{-1/3} - 0.98d^{-1/3}\right] \quad (5)$$

and

$$\sigma_t^2 = 2\lambda^2 r_o^{5/3} \left[0.179D^{-1/3} - 0.145d^{-1/3}\right] \quad (6)$$

where λ is the wavelength and r_o is the Fried Parameter. Variance can be calculated from a series of video frames taken at specified intervals, and r_o can be calculated from equations (6) and (7). The seeing value can be calculated by entering the values of λ and r_o into equation (5).

8 RESULTS AND DISCUSSION

The observation was conducted at the Universitas Ahmad Dahlan Observatory in April, May, and September 2019. Table 1 shows the time of observation and related star. We can see that the zenith distances for the six stars are similar to each other. Hence, we can compare the condition of the atmosphere above the observatory by using different stars and time.

Table 1: Time of Observation

Time	Stars	Angular Diameter (")	Zenith (^{o})
10-04-2019	Procyon	0.063	29
10-04-2019	Sirius	0.0121	27
18-05-2019	Spica	0.0017	22
18-09-2019	Altair	0.0059	25
18-09-2019	Nunki	0.0013	23
18-09-2019	Vega	0.0066	29

The DIMM results gave the number of seeing data for number of frames. Those data can be grouped to be counted as the amount of data on the particular value of seeing. The value of seeing on Procyon, Sirius, Spica, Altair, Nunki, and Vega stars can be seen in Figure 8 as the distribution graph.

Seeing characteristics is determined by analyzing the dominant value of seeing in the 10 seconds time interval. Narrower seeing value distribution, better seeing condition. Since there is only one maximum

count of seeing value [21, 26], the dominant values of seeing of Procyon, Sirius, Spica, Altair, Nunki, and Vega are 0.2 arc seconds, 0.3 arc seconds, 0.1 arc seconds, 1.3 arc seconds, 1.3 arc seconds, and 1.5 arc seconds, respectively. As we see in table 1, we can compare the seeing value to the stars' angular diameter. The range of the ratio between seeing to the angular diameter is between 3.175 to 1000. Table 1 also shows the time of observation. The April observation is relativity better than the September observation. The changing of observation quality is due to the high dynamics motion in the atmosphere during the September observation. The weather at the observatory started to change from the dry season to the rain season. The weather is also the factor to be considered on the lunar crescent observations [27]. Hence, we need to provide the weather condition and the prediction and the seeing characteristics for observers to get high-quality data. Despite the weather constraint, this result is a vital feature to guide the astronomers to perform observation at the Universitas Ahmad Dahlan.

9 CONCLUSIONS

Based on research that has been carried out measuring seeing at the UAD observatory using the DIMM method with the Celestron C6-N telescope produces excellent characteristics on April 10^{th}, 2019, with a Procyon star with a value of 0.2 arc seconds and on September 18^{th}, 2019, Vega star with a value of 1.6 arc seconds. The weather condition influences the value at the time of observation.

ACKNOWLEDGEMENTS

This work was supported by the Internal Research Funding of Universitas Ahmad Dahlan. The Observatorium UAD was also giving full access to the facility.

AUTHOR

1 Ricka Tanzilla
From :
(1) Magister Pendidikan Fisika, Universitas Ahmad Dahlan

2 Yudhiakto Pramudya
Dari :
(1) Magister Pendidikan Fisika, Universitas Ahmad Dahlan

3 M. Khairul Ardi
Dari :
(1) Magister Pendidikan Fisika, Universitas Ahmad Dahlan

4 Okimustava
Dari :
(1) Magister Pendidikan Fisika, Universitas Ahmad Dahlan

References

1. Mahasena P, Akbar EI, Yusuf M, Hidayat T, Dermawan B, Herdiwijaya D, et al. Pengukuran Seeing di Sekitar Gunung Timau, Nusa Tenggara Timur. 2013;p. 2–4.
2. Cherubini T, Businger S, Lyman R, Chun M. Modeling optical turbulence and seeing over Mauna Kea. Journal of Applied Meteorology and Climatology. 2008;47(4):1140–1155.
3. Floyd DJE, Thomas-Osip J, Prieto G. Seeing, wind, and outer scale effects on image quality at the magellan telescopes. Publications of the Astronomical Society of the Pacific. 2010;122(892):731.
4. Aime C, Roddier F. Imaging through turbulence with telescope arrays. Optics Communications. 1976;19(1):57–60.
5. Ahmad N, Loon CW, Syukor MS, Haron S, Zainuddin MZ, Tahar MR. The astronomical seeing measurements at Langkawi National Observatory. In: 2015 International Conference on Space Science and Communication (IconSpace). IEEE; 2015. p. 339–342.
6. Kornilov V, Tokovinin A, Shatsky N, Voziakova O, Potanin S, Safonov B. Combined MASS–DIMM instruments for atmospheric turbulence studies. Monthly Notices of the Royal Astronomical Society. 2007;382(3):1268–1278.
7. Danesh A, Khosroshahi HG, Javanmardi B, Molaeinezhad A, Abedini Y, Altafi H, et al. Iranian national observatory project: seeing measurements at mount Gargash. Experimental Astronomy. 2019;47(1-2):145–160.
8. Tanzilla R, Jauhari I, Pramudya Y. Measurement Eccentricity the Moon's Orbit with Image Analysis Technique by Using Tracker Software. Indonesian Review of Physics. 2018;1(1):19–25.
9. Raisal AY, Pramudya Y, Okimustafa O, Muchlas M. The moon phases influence on the beginning of astronomical dawn determination in Yogyakarta. In: International Journal of Science and Applied Science: Conference Series. vol. 2. UNS; 2017. p. 1–7.
10. Kolář J, Prudký J. How to measure seeing. European Association for Astronomy Education (EAAE), Online course available: http://www eaaeastronomy org/catchastar/images/2015/18_How_to_measure_seeing pdf;.
11. Hege EK, Jefferies SM, Lloyd-Hart M. Computing and telescopes at the frontiers of optical astronomy. Computing in Science & Engineering. 2003;5(6):42–51.
12. Tritton DJ. Physical fluid dynamics. Springer Science & Business Media; 2012.
13. Moulick R. Good Morning Science. India. 2017;p. 1–7.
14. Bakker A. Lecture 9-kolmogorov's theory applied computational fluid dynamics. Educational material© Fluent Inc. 2002;.
15. Darmawan S. Pengembangan model turbulen RNG KE untuk aplikasi CFD pada runner cross flow dalam komponen turbin gas mikro bioenergi proto X 2a= RNG KE turbulence model development for cfd application on cross flow runner of a proto x 2a bioenergy micro gas turbine. 2015;.
16. Martin HM. Image motion as a measure of seeing quality. Publications of the Astronomical Society of the Pacific. 1987;99(622):1360.
17. Fried DL. Statistics of a geometric representation of wavefront distortion. JoSA. 1965;55(11):1427–1435.
18. Tokovinin A. From differential image motion to seeing. Publications of the Astronomical Society of the Pacific. 2002;114(800):1156.
19. Ruler M. How to Find FWHM; 2017. Available from: https://sciencing.com/fwhm-5370769.html.
20. Rana T. Full width at half maximum; 2018. Available from: https://en.wikipedia.org/w{%}5C/index.php?title=Full{_}width{_}at{_}half{_}maximum{&}oldid=864676968.
21. Martinez P, Kolb J, Sarazin M, Tokovinin A. On the difference between seeing and image quality: when the turbulence outer scale enters the game. ESO Messenger. 2010;141:5.
22. Vernin J, Munoz-Tunon C. Measuring astronomical seeing: the DA/IAC DIMM. Publications of the Astronomical Society of the Pacific. 1995;107(709):265.

23. Brandt PN. Measurement of solar image motion and blurring. Solar Physics. 1970;13:243–246.
24. Stock J, Keller G. Astronomical seeing. tele. 1961;p. 138.
25. Sarazin M, Roddier F. The ESO differential image motion monitor. Astronomy and Astrophysics. 1990;227:294–300.
26. Douglass AE. Scales of seeing. 1898;.
27. Hidayat T, Mahasena P, Dermawan B, Herdiwijaya D, Setyanto H, Irfan M, et al. Developing information system on lunar crescent observations. Journal of Mathematical and Fundamental Sciences. 2010;42(1):67–80.

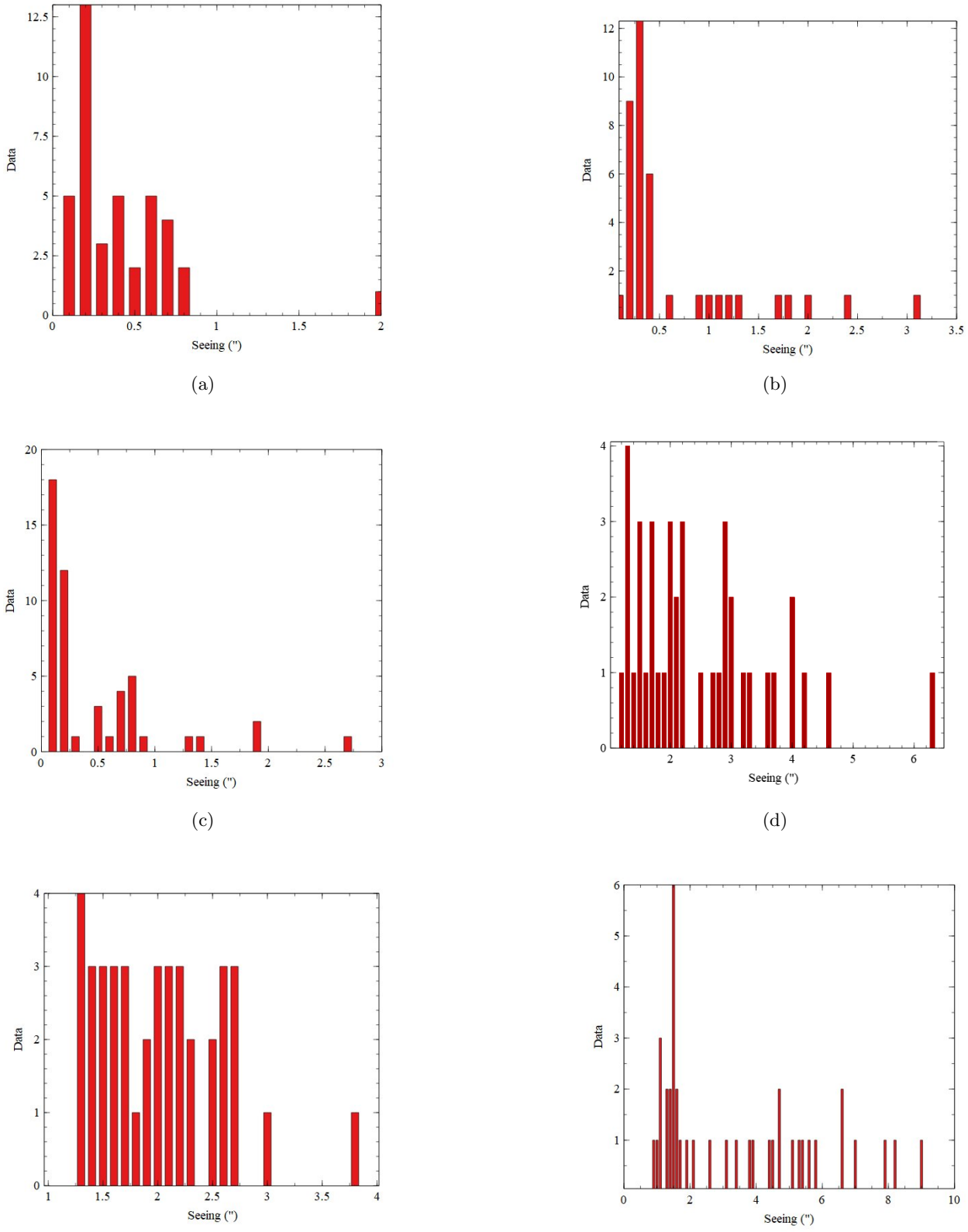

Figure 2: (a) The distribution graph of seeing Procyon ,(b) seeing Sirius,(c) seeing Spica, (d) seeing Altair,(e) seeing Nunki, dan (f) seeing Vega.